AMERICAN UNIVERSITY OF BEIRUT

THE ASSESSMENT AND ENHANCEMENT OF THERMAL COMFORT IN THE MAKASSED SCHOOLS, BEIRUT

by
MICHEL MARIO ZAKHARIA

A thesis
submitted in partial fulfillment of the requirements
for the degree of Master of Engineering
to the Department of Mechanical Engineering
of the Maroun Semaan Faculty of Engineering and Architecture
at the American University of Beirut

Beirut, Lebanon
April 2022

AMERICAN UNIVERSITY OF BEIRUT

THE ASSESSMENT AND ENHANCEMENT OF THERMAL COMFORT IN THE MAKASSED SCHOOLS, BEIRUT

by

MICHEL MARIO ZAKHARIA

Approved by:

Aram Yertzian

Digitally signed by Aram Yeretzian
DN: cn=Aram Yeretzian, o=American University of Beirut, ou, email=ay10@aub.edu.lb,c=LB
Date : 2022.05.05 21 :11 :10+03'00'

Prof. Aram Yeretzian, Assistant Professor Architecture and Design	Signature Advisor
Dr. Issam Lakkis, Professor Mechanical Engineering	Signature Co-Advisor
Dr. Kamel Aboughali, Professor Mechanical Engineering	Signature Member of Committee

Date of thesis defense: April 29,2022

AMERICAN UNIVERSITY OF BEIRUT

THESIS RELEASE FORM

Student Name:	Zakharia	Michel	Mario
	Last	First	Middle

I authorize the American University of Beirut, to: (a) reproduce hard or electronic copies of my thesis; (b) include such copies in the archives and digital repositories of the University; and (c) make freely available such copies to third parties for research or educational purposes:

☐ As of the date of submission

☒ One year from the date of submission of my thesis.

☐ Two years from the date of submission of my thesis.

☐ Three years from the date of submission of my thesis.

Michelzakharia 11/05/2022

Signature Date

ACKNOWLEDGEMENTS

I would like to thank my advisors Dr Issam Lakkis and Dr Aram Yeretzian for the constant support and guidance throughout the last two years. The weekly meetings were extremely helpful in improving my knowledge in the fields of machine learning and building energy modeling.

I would also like to thank Dr Kamel Aboughali for being in my thesis committee and providing his helpful insight regarding heat transfer.

Finally, I would like to thank my family and friends for their encouragement and support. Namely, my sister Gloria Zakharia and my friend Michelle Ghosb Dit Ghosn who provided me with moral support throughout the research process.

ABSTRACT

OF THE THESIS OF

Michel Mario Zakharia for Master of Engineering
Major: Mechanical Engineering

Title: The Assessment and Enhancement of Thermal Comfort in the Makassed Schools, Beirut

Improving the thermal behavior of old buildings' external envelope to meet current standards is a subject that every country needs to tackle when talking about eco-efficient building design. In cities, buildings constructed several decades ago account for a substantial percentage of the total residential buildings. The same applies to the Mediterranean city of Beirut, the capital of Lebanon. Retrofitting the external walls of old buildings aims to decrease the energy consumed to maintain comfortable conditions inside the residential space. This study assesses the thermal behavior of four different walls located in the Makassed Schools in Beirut, three are made of sandstone and the other is made out hollow concrete blocks. The goal of this study is to propose modifications on the current constructions to enhance the thermal comfort inside of each classroom. To do so, recorded temperature data were analyzed, and the thermal behavior of the walls was described using the thermal time lag and decrement factors. Furthermore, energy models for the four spaces were created using the OpenStudio application and the Sketchup plugin. These models were calibrated according to the standards set by ASHRAE and validated for a full year. Subsequently, unretrievable construction data, mainly the density and the specific heat of the building envelope, were estimated using the Markov Chain Monte Carlo method by the means of the interface linking python and the building energy simulator EnergyPlus. The calibrated models were used as a basis to compare the thermal performance of various passive energy saving techniques available in the Lebanese market. The results show that extruded polystyrene, double window glazing, and rock wool insulations are readily available options capable of significantly enhancing the thermal comfort of the classes without relying on mechanical ventilation.

TABLE OF CONTENTS

ILLUSTRATIONS

Figure

TABLES

Tables

CHAPTER I

INTRODUCTION

On a global scale, the building sector accounts for 30-40% of the global energy consumption (Hema et al., 2020). Therefore, while discussing the issues of global warming and climate change, mitigating the energy consumption of buildings is a subject of high priority. In Beirut, most of the constructions were made before 1990, and were subjected to heavy damage through the various catastrophic events that struck the country. Public schools in Lebanon are notorious for having low student thermal comfort and outdated facilities. Indoor thermal comfort is essential for the health and productivity of building occupants, especially those who spend long periods in indoor environments, such as teachers and students. These establishments do not use mechanical ventilation systems; therefore, the thermal conditions inside the classrooms are only determined by the prevalent climate in each season. Climate responsive building design is essential to ensure that the students and the staff work under comfortable conditions regardless of the outside temperatures. The Lebanese climate leans toward being hot most of the year, having warm fall and spring a mild winter, and a long summer that drags until the end of October. In an age where people are forced to spend most of their time indoors, achieving a comfortable thermal space indoors is essential for everyday life. Thermal comfort conditions refer to the temperature range where the inhabitants of a certain space do not feel either hot or cold. Typically, thermal comfort is attained at temperatures ranging between 19-25℃ as defined by the American Society of Heating, Refrigerating, and Air-Conditioning Engineers (ASHRAE). Thermal comfort is a subjective metric therefore, various formulas can be found in the literature that aims to predict the human's response to the prevailing

thermal conditions in a certain space (Albatayneh et al., 2018; Nicol & Humphreys, 2002). Achieving comfortable thermal environments indoors is the main driver for the significant energy consumption registered from indoor operations. This is done through the installation of heat ventilation, and air conditioning (HVAC) systems inside each building. Thermal discomfort occurs in buildings if the energy exchange between the indoors and the outdoors is not taken into consideration in the design and construction phase. Addressing this issue later in the building's life is costly, as the main thermal components are already set. The choice of building materials is an essential factor in the energy needs of the indoor space. Consequently, addressing thermal comfort issues needs a complete remodeling of the existing building which is both not economical and not practical (Latha et al., 2015). Tackling the issue of renovating a pre-existing building, especially old ones to have better comfort conditions is a challenging task especially, in a country like Lebanon. Building codes in Lebanon do not enforce the renovation of pre-established buildings. Indoor thermal comfort is essential for the health and productivity of building occupants, especially those who spend long periods in indoor environments, such as teachers and students. In this study, four different locations in the Makassed Schools in Beirut were monitored throughout the year 2019. Using these data, the objective is to develop valid thermal models for each of the spaces as a basis for analysis. Then, various building materials will be tested to enhance the thermal conditions in the classrooms in an eco-effective manner under natural ventilation.

CHAPTER II

LITERATURE REVIEW

Green building design relies on the effective use of building materials to regulate the thermal transfer in the indoor environment. In a working space, the thermal comfort of the occupants heavily influences the workers' well-being and productivity. In a broader sense, green buildings aim to ensure the thermal comfort of the occupants while minimizing the mechanical energy spent on HVAC systems. The standards of thermal comfort were set by the American Society of Heating, Refrigerating and Air-Conditioning Engineers (ASHRAE) in Standard 55 which gets updated every few years (Turner et al., 2010). As a concept, thermal comfort is a psychological term that refers to the state in which someone is neutral about the thermal conditions surrounding them. Since thermal comfort is not a measurable metric, and rather it is a subjective one, there cannot be a range of comfort temperature that applies to everyone (Turner et al., 2010). For instance, someone living in Canada will find the Mediterranean climate to be too hot while someone living in Lebanon will find Canada's climate to be too cold. Consequently, various models are available to predict the thermal comfort in a certain space the most notable being the predicted mean vote model (PMV), and the adaptive thermal comfort models (Albatayneh et al., 2018; Nicol & Humphreys, 2002). The PMV model assigns a value for each thermal condition, ranging from -3 for Cold to +3 for Hot while thermal comfort is achieved in the range between -0.85 to +0.85. This model includes six major variables which are: the mean radiant temperature, the relative humidity, the metabolic rate and clothing insulation of the occupants, the air temperature, and the air velocity. The PMV model is by no means a perfect one, it has a set of limitations that inhibit its effectiveness, especially in naturally ventilated

buildings. The main challenge of the PMV model is that it fails to consider the psychological factors that affect the occupants and only tackles the physics of heat transfer. This model is most successful in spaces that are mechanically ventilated because the temperature distribution in the room is uniform. To tackle the limitations of the PMV model in free-running buildings, adaptive thermal comfort models were developed as a more general model that accounts for the response of the occupants to the changing weather conditions (Albatayneh et al., 2018; Nicol & Humphreys, 2002). Experimental investigations have shown that the adaptive thermal model offers a wider range of thermal comfort temperatures. In their study Albatayneh et al., (2018) have found that adaptive thermal comfort models reduce the mechanical energy needed in naturally ventilated buildings by 20% while any discomfort can be solved via low energy alternatives.

The energy demand of a building is the result of the interaction between several parameters such as the building materials, the ventilation process, the windows, and building orientation. Numerous studies have dealt with finding eco-efficient building materials under various climate conditions. Homod et al., (2021) have compared the thermal performance of aerated concrete blocks in modern houses to the thermal performance of vernacular houses built using clay and straw. In the case study conducted in Iraq, they have found that the clay and straw houses were able to save 48% of the HVAC energy used in the concrete houses. Hema et al., (2020) studied the effect of using compressed earth blocks on the discomfort of the occupants in hot climates using building energy simulation. In combination with two insulations layers, the use of compressed earth blocks as thermal mass reduced the cooling loads compared to concrete blocks. Overall, the study concluded that a double-layered wall offers great

opportunities to enhance thermal comfort in naturally ventilated buildings. In a similar study Jannat et al., (2020) examined the effect of different building materials, orientations, and insulations on thermal comfort in tropical climates. The aerated concrete blocks have performed the best under the study's conditions due to their low U-value and thermal diffusivity. The envelope of the building is the main medium of heat exchange between the building and the exterior environment, therefore proper control of the thermal properties of its materials is necessary to achieve thermal comfort. Materials with low U-value and thermal diffusivity tend to decrease the cooling loads and temperature fluctuations in the indoor space(Hema et al., 2020; Jannat et al., 2020; Latha et al., 2015).

Another factor that is essential for thermal comfort is the ventilation of the building. In free-running buildings air is circulated through the doors and windows of the indoor space. The lack of ventilation leaves the heat gained through the day inside the space which results in overheating of the occupants(Latha et al., 2015). Windows are a source of heat gain and ventilation indoors. The type of glass, it's glazing, and its operations schedule can enhance or worsen the thermal comfort of the occupants. Kumar et al., (2017) have studied the effect of different window glazings combined with several building materials on a house in India. Bronze tinted glass and a mud-brick envelope have proven to be the most energy-efficient as it reduces the cooling load during the summer. Another eco-effective building practice is the use of vegetation to improve the energy uptake of the indoor space. In the summer, plants can provide shade and reduce the solar exposure of the space while in the winter it shields the building from the wind reducing the heating load required indoors. Haggag et al., (2017) has studied the energy and economic performance of a plant shaded façade. The payback

time of the façade was calculated to be 10 years while it was able to reduce the indoor temperatures by 2℃ on average and the cooling load by 0.3 MWh.

Experimental investigation of buildings is not always an available option when studying the thermal behavior of buildings. Building energy simulation softwares are used to build accurate models to predict the behavior of space in a certain period. The simulation process consists of: modeling the space, calibrating the model, and simulating the calibrated model. Bagnasco et al., (2018) have modeled the electrical engineering department at the University of Genova using the Energy Plus software. The model included the electrical supply, air conditioning system, and heat supply. The model was calibrated using the actual power consumption of the building to minimize the error between the simulation results and the measured data. This model was able to predict the energy performance and the electric demand of the building accurately. Jradi et al., (2017) modeled a building located at the University of Denmark. Using OpenStudio and Energy Plus the model was created and calibrated against utility data that correspond to a the study period. Retrofit packages were proposed and a PV system was chosen to decrease the energy consumption of the building. Simulating existing buildings, especially old constructions is a challenging task as it is coupled with high level of uncertainty regarding the material composition if the building envelope. Determining the thermal properties of the materials in such cases may not be feasible. Therefore, uncertainty analysis are carried out in order to determine the sensitivity of the model to each variable (Chong et al., 2015; Corrado & Mechri, 2009; Prada et al., 2018). Monte Carlo based algorithms are being introduced as mean to tackle the uncertainty associated with building energy simulations. Prada et al., (2018) has used the simulator TRANSYS to produce probability density functions for various building

materials that have unkown thermal properties. The thermal properties of concrete and timber were fitted into a normal, lognormal and asymetric distributions. Chong et al., (2015) have implemented an uncertainty analysis on 649 variables in Energyplus. The algorithim was based on the Monte Carlo method, and provided probabilistic estimations of the studied variables. However these results were not final, as the assumed Guassian distribution may not be representative of the actual uncertainty propagation.

A. Limitations of the Current Literature

After an extensive review of the available literature, the following limitations were identified:

- The thermal behavior of spaces made of sandstone walls is not studied in the literature.
- Thermal renovation of old buildings in Mediterranean climate is not extensively researched. There are no defined alternatives that can enhance the energy performance of those buildings in the Mediterranean climate.
- The data collection process regarding the pre-existing building envelope is unclear.
- Building energy models of existing spaces do not tackle the unknown thermal parameters and composition of the opaque envelope.
- The process of calibrating energy models of old buildings, with unknown thermal properties is not explicitly defined.

B. Research Objectives

This study aims to understand the thermal behavior of historic buildings in a Mediterranean climate. The objective is to build accurate energy models for four different spaces in the Makassed schools, these models will be used as a basis for enhancing the thermal comfort of those spaces. Furthermore, the goal is to select the best materials and parameters that can enhance the thermal comfort of those spaces. The following questions will be answered in this study:

- How do sandstone walls affect the thermal space indoors under different weather conditions throughout the year?
- Is it possible to infer unknown building properties, using BEM and experimental data?
- What are the best eco-friendly modifications to the sandstone and concrete envelopes that enhance the thermal comfort of the occupants?

CHAPTER III

MATERIALS AND METHODS

A. Methodology Program

The steps to solve the previously defined research problem are as follows. First on site data was recorded including temperature measurements, construction surveys, occupancy schedule, and dimensions of the studied spaces. Then these data were translated to a BEM and calibrated using Bayesian statistics. Finally, enhancement scenarios were proposed to enhance the thermal comfort of the spaces. The methodology program is represented in Figure 1.

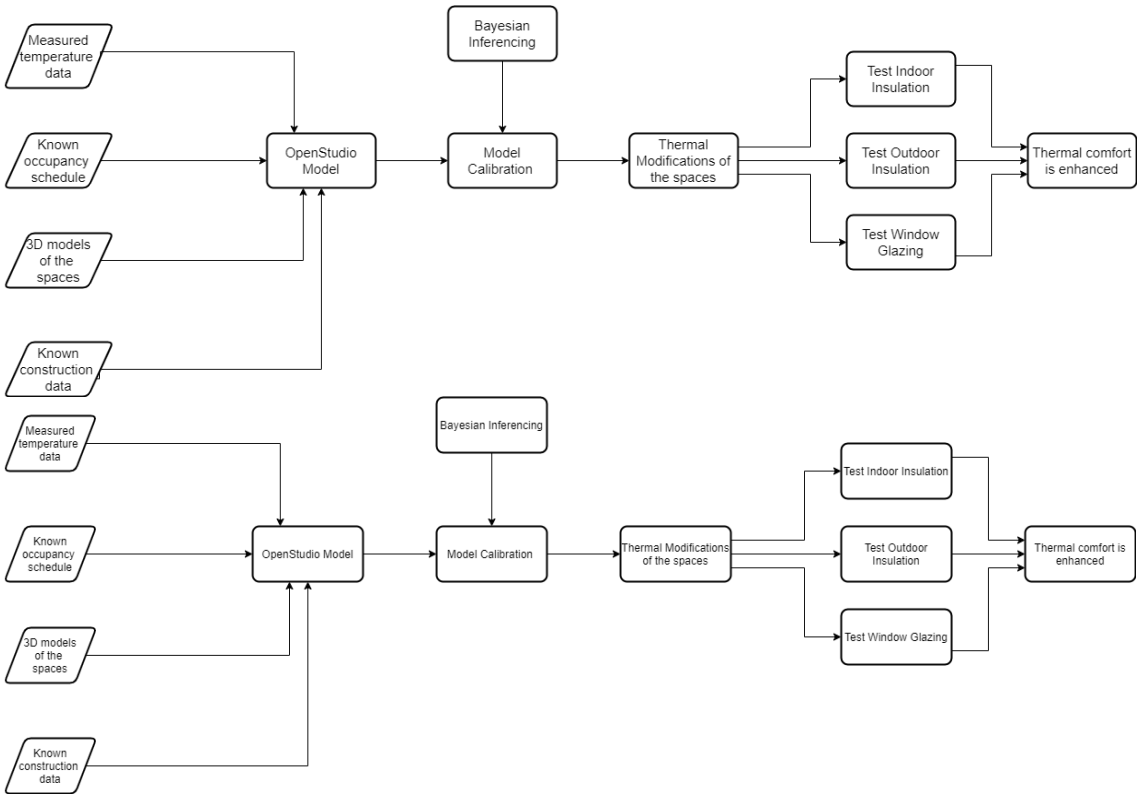

Figure 1 Methodology Diagram

B. Site Description

Characterizing the different spaces is the first step in developing a reliable building energy model. Such models require various inputs including but not limited to a 3D

model of the building, construction properties, occupant's schedule, existing ventilation systems, and an appropriate weather file. These variables were reported directly from the Makassed school with assistance from the construction and renovation staff. Visiting the school allowed the identification of different construction methods relevant to each of the four spaces. The three spaces studied in the Makassed schools are located in two adjacent areas in Beirut: Barbir and Bachoura. The construction properties of each of the walls studied are presented in Table 1, and the layouts of the spaces containing these walls are presented in Figure 2.

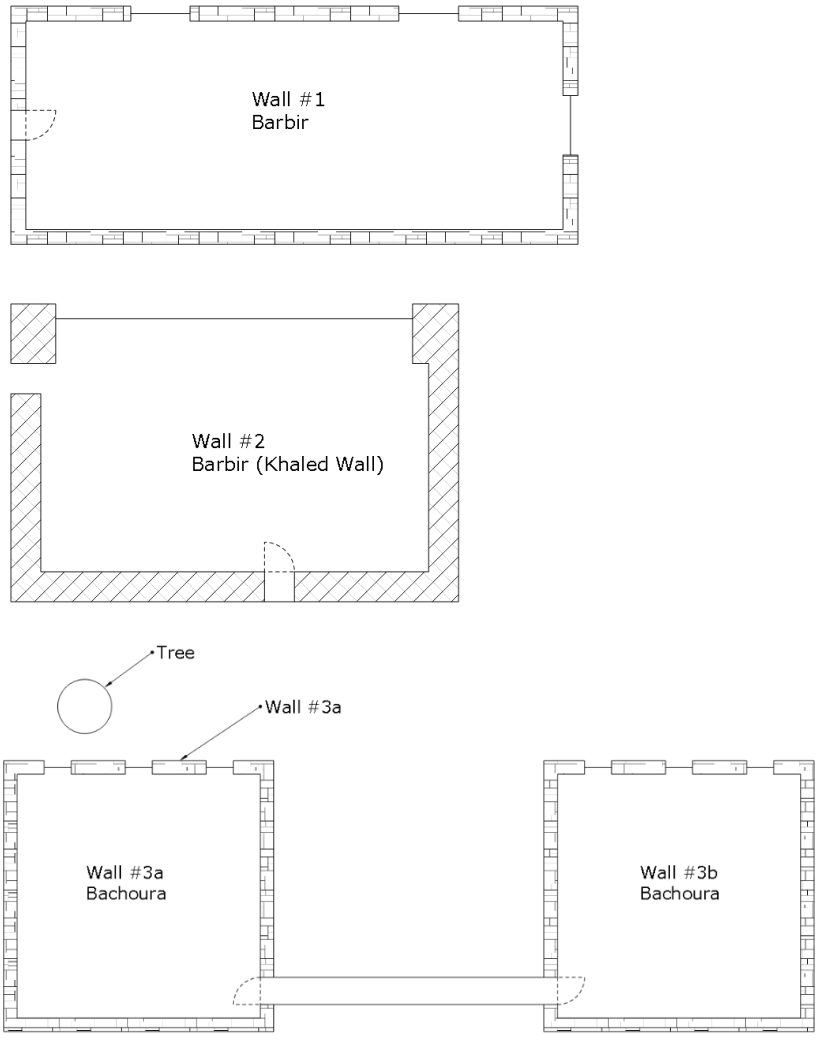

Figure 2 Layout of the Studied Spaces

Table 1 Properties of the Studied Walls

Property	Wall #1	Wall #2	Wall #3a (Tree)	Wall #3b (No tree)
Construction Date	1920	1960	1860	1860
Plaster	Lime (Interior)	Cement	Lime	Lime
Material	Sandstone	Hollow concrete blocks	Sandstone	Sandstone
Thickness	27.5cm	30cm	31cm	31cm

From the Khaled Bin Walid School, two walls are studied named Wall #1 and Wall #2. The former is located in the Nursery building of the school while the latter is located in the primary school building of the school. The third wall studied is located in the Bachoura, mainly used as a training center on the first floor of the building. A gypsum false ceiling construction is present in the rooms containing Wall #1 and Wall #3a. In contrast, Wall #3a's room had a plenum construction consisting of a hanging ceiling at a height of 3m and the real ceiling at a height of 6m. Plenum constructions are used to enhance the circulation of air in the space for heat ventilation and air conditioning applications (Brackney et al., 2018). The space containing Wall #2 has a concrete construction with concrete slabs supporting he ceiling from below. Even though, each of the studied spaces has different shading configurations for the windows, the most notable difference between Walls #3a and #3b is the presence of a giant tree in front of Wall #3a.

C. Thermal Properties

The thermal behavior of a building is captured by the thermal time lag and decrement factors. Therefore, a proper representation of the thermal properties of the walls requires a specific choice of the study period. These thermal parameters can be

determined with respect to the prevalent thermal stress during the season. Three distinct periods can be delaminated through the plot of the ambient temperature of each space during the year (Cherier et al., 2019). February was taken as the month with the lowest heat stress, April was taken as the month with the average heat stress and July was taken as the month with the maximum heat stress. Asan (2006) defines the thermal time lag as follows:

$$\varphi = \begin{cases} t_{T_i^{max}} > t_{T_e^{max}} \rightarrow t_{T_i^{max}} - t_{T_e^{max}} \\ t_{T_e^{max}} > t_{T_i^{max}} \rightarrow t_{T_e^{max}} - t_{T_i^{max}} + P \\ t_{T_i^{max}} = t_{T_e^{max}} \rightarrow P \end{cases}$$

Where:

- P is the period of the sinusoidal function,
- $t_{T_i^{max}}$ is the time at which the inside surface temperature peaks
- and $t_{T_e^{max}}$ is the time at which the outside surface temperature peaks through the day.

These calculations rely on the harmonic representation of the temperature function (Asan, 2006; Babu et al., 2014; Bevilacqua et al., 2018):

$$T(t) = \bar{T} + \sum_{k=1}^{n} T_k = \bar{T} + \sum_{k=1}^{n} |T_k| \sin(\omega_k t + \varphi_k)$$

Where:

- $\bar{T}$ represents the mean value of the surface temperature studied,
- $|T_k|$ is the amplitude of the sine wave,
- ω_k is the angular frequency of the function,
- n is total the number of harmonic functions
- and φ_k is the phase angle of the temperature wave.

The thermal time lag and decrement factor are usually calculated under stable conditions where the fluctuation in the heat flux is minimal (Asan, 2006; Babu et al., 2014; Cherier et al., 2019; Toure et al., 2019). As a result, an unsteady state analysis of the building wall material will need some modifications and corrections to get representable values of both parameters. The Fourier series is used to normalize the data into a sinusoidal function. The harmonic evaluation treats the experimental temperature data as a discrete Fourier series which normalizes the data using the mean, maximum and minimum surface temperatures (Babu et al., 2014; Gasparella et al., 2011).

The time lag is therefore given by:

$$\tau = \varphi_{k,i} - \varphi_{k,e}$$

and its calculation was done following the procedure of Asan (2006). Consequently, the decrement factor is defined as:

$$DF = \frac{|T_{k,i}|}{|T_{k,e}|}$$

In addition to the harmonic normalization of the temperature data, a noticeable baseline shift was observed in the graphs. The function “detrend” was used to remove the meaningless polynomial trends and a comparison between the normal data and the detrended one was done for the three months. The decomposition of the real time trends into a harmonic function was carried out using a Fast Fourier Transform analysis on MATLAB. First the average daily surface temperature was removed from the hourly data, then it was analyzed using the Fast Fourier Transform fft() function, that determines the peak and the magnitude of the transformed data (Babu et al., 2014; Gasparella et al., 2011). The period of the function is calculated using the findpeaks() function from the signal processing toolbox.

D. Building Energy Simulation

In this study, the OpenStudio software will be the basis of the building energy simulations. First released in 2010, OpenStudio was developed by the National Renewable Energy Laboratory as an application based on the building simulation tool Energy plus and the Department of Energy (DOE)'s daylighting radiance engine (Brackney et al., 2018). Building Energy Modeling (BEM) relies on two characterization steps: Structural characterization and Functional characterization. The structural characterization of the building defines the 3D model of the school spaces and assigns the relevant materials to its components. This step is mostly done using Sketchup pro and the OpenStudio SketchUp plugin. Subsequently, the functional characterization refers to the modeling of the HVAC systems along with the thermal behavior of the occupants and equipment (Bagnasco et al., 2018). During the period when the temperature data were collected, the country's circumstances and later the Corona Virus outbreak has made these spaces unoccupied. As for the simulations, it is assumed that the functional parameters of the different buildings have little to no contribution to the thermal behavior in the studied spaces.

Once the spaces are properly modeled, an appropriate EPW weather file is needed to launch the Energy Plus simulations. The weather properties file was made using the open-source software Elements. While the relevant parameters were recorded by a weather station located at the American University of Beirut (AUB). The measured data were measured and included: yearly internal and external surface temperatures of the walls, indoor air temperature, a week of heat flux measurements, and estimations of the product of the density and the specific heat, the thermal conductivity, and the heat transfer coefficient U.

1. Model Calibration

First, the measured internal surface temperature is calibrated against the simulated internal surface temperature of the walls. It is also assumed that the internal surface temperature of the wall is a better representative of the thermal properties of the wall than the external surface temperatures due to the uncontrollable nature of the outdoor spaces. This step of the calibration aims to get an estimate of the unknown values of the density and the specific heat of the wall layers. Second, the measured indoor ambient temperature serves as a calibration basis for the thermal behavior of the other parts of the envelope mainly the floor and ceiling materials. The "goodness" of the model calibration is judged by the coefficient of variation of the root mean squared error (CVRMSE) and the net mean bias error (NMBE). These parameters are given by the following equations (Brackney et al., 2018):

$$NMBE = \frac{100}{\bar{y}} \times \frac{\Sigma(y_i - \hat{y}_i)}{n} \; CVRMSE = \frac{100}{\bar{y}} \times \sqrt{\frac{\Sigma(y_i - \hat{y}_i)^2}{n}}$$

Where:

- y_i represents the measured data,
- $\hat{y}_i$ represents the simulated data point,
- $\bar{y}$ is the mean of the measured data,
- and n is the total number of measured sample points.

According to Brackney et al., (2018), ASHRAE regulates, in Article 14, the values of the CVRMSE and the NMBE. The values of the CVRMSE and the NMBE need to be below 30% and 10% respectively.

2. Uncertainty Analysis

The properties of the opaque materials, for which no temperature measurements were taken, were calculated using the Markov Chain Monte Method (MCMC). This approach generates thousands of samples from a posterior distribution, typically a Gaussian distribution, to quantify the uncertainty in the model parameters and therefore result in better model calibration. The algorithm used to perform Bayesian calibration of the EnergyPlus models is the Metropolis-Hastings algorithm (MH). Being a subclass of the MCMC algorithms, the Metropolis algorithm draws samples from a posterior probability distribution, knowing only a function proportional to it. This algorithm generates Markov Chain candidates from a proposal distribution that are accepted or rejected according to a specific rule.

The calibration was set up in the programming language Python. The premade OpenStudio models were translated into EnergyPlus files, after that the simulations were conducted using the Python package Eppy. This package allows iterating the properties of the building materials, mainly the density and the specific heat, which produces the probability distribution of those variables.

E. Thermal Comfort Assessment and Enhancement

Once the calibrated models were made, the OpenStudio application is used to assess the thermal comfort of the different spaces. The application houses a variety of thermal comfort algorithms ranging from traditional computations to modern adaptive algorithms. Theoretical scenarios were proposed to simulate the occupancy of the school under normal conditions aiming to assess how comfortable are the spaces during a normal year. These scenarios, coupled with the adaptive thermal comfort models serve as a basis for proposing enhancements to the current constructions. This study explored

three main renovation strategies that are readily available in the Lebanese market which are insulation, double-wall construction, and window glazing.

1. Insulation

The insulation data were adapted from the Kilzi construction company and include the thermal properties of natural Cork insulation, Stone Wool insulation, and Expanded Polystyrene (EP). The extruded polystyrene (XPS) data was adapted from the DuPont company since Styrofoam™ XPS is an appealing insulation in terms of its thermal properties.

Table 2 Thermal Properties of the Chosen Insulation Materials

Insulation	**Density** $(\boldsymbol{Kg/m^3})$	**Thickness (mm)**	**Specific heat** $(\boldsymbol{KJ/Kg}°C)$
Cork insulation	120	10-320	1.67
Stone Wool insulation	94	30-200	1
Expanded Polystyrene	32-35	20-100	1.3
Extruded Polystyrene	38	20-100	1.5

a. Cork Insulation:

Cork insulation is obtained from peeling the bark of trees. It has the following properties:

- High thermal resistance.
- Noise resistance.
- Reduced environmental impact.

b. Stone-wool Insulation:

Stone-wool insulation is produced from mineral rocks with the addition of wool fibers. This type of insulation is characterized by:

- Excellent thermal insulation
- Fire and sound resistance
- Practicality, it can be cut and installed according to the users' demands

c. Expanded Polystyrene:

The following are the advantages and disadvantages of expanded polystyrene insulation.

- Advantages:
    - Low weight, high compression strength.
    - High insulation value, constant over time.
    - Easy, clean, and safe to work with.
- Environmental Concerns:
    - Made of fossil fuels.
    - Consumes high amounts of energy in production.

d. Extruded Polystyrene:

DuPont Styrofoam branded XPS insulation is a product designed to minimize the effect of the construction materials on carbon dioxide emissions by providing high thermal and moisture resistance. In terms of sustainability, this insulation has low global warming potential, and is made from 20% recyclable materials.

2. Double Window Glazing

The double window glazing consists of two separate glass layers in the window. It helps on improving the thermal performance of the window. The thermal properties of the glazing are summarized in Table 3.

Table 3 Thermal Properties of Different Glazing Types

Window Type	**U-value in W/m^2K**	**Solar absorbance**
Single glazing	4.8	0.8
Double glazing	2.5	0.6

3. Thermal comfort enhancement scenarios

The previously listed materials will be tested on the respective spaces using the OpenStudio calibrated models. For each wall, all the different types of insulations will be tested either on the inside or the outside and will further combine the results with the double window glazing. In each case, the best-performing insulation will be tested based on its location as shown in Figure 3,4 and 5.

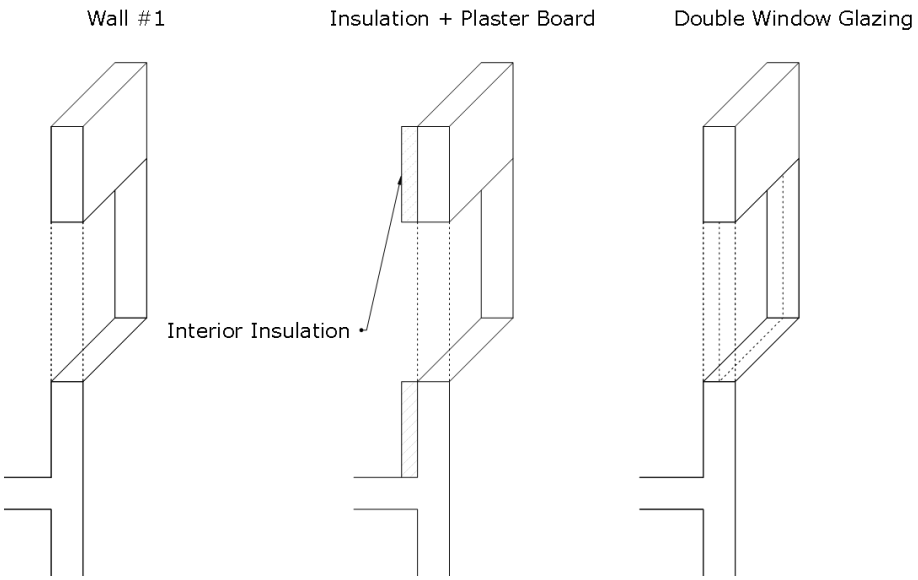

Figure 3 Nursery Enhancement Scenarios

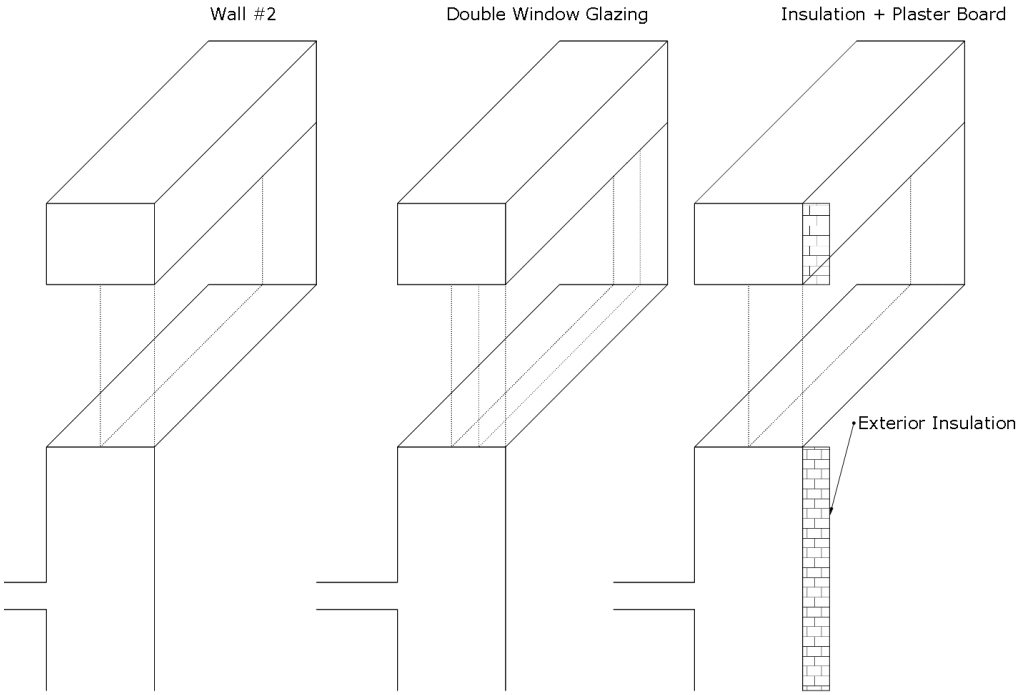

Figure 4 Khaled Enhancement Scenarios

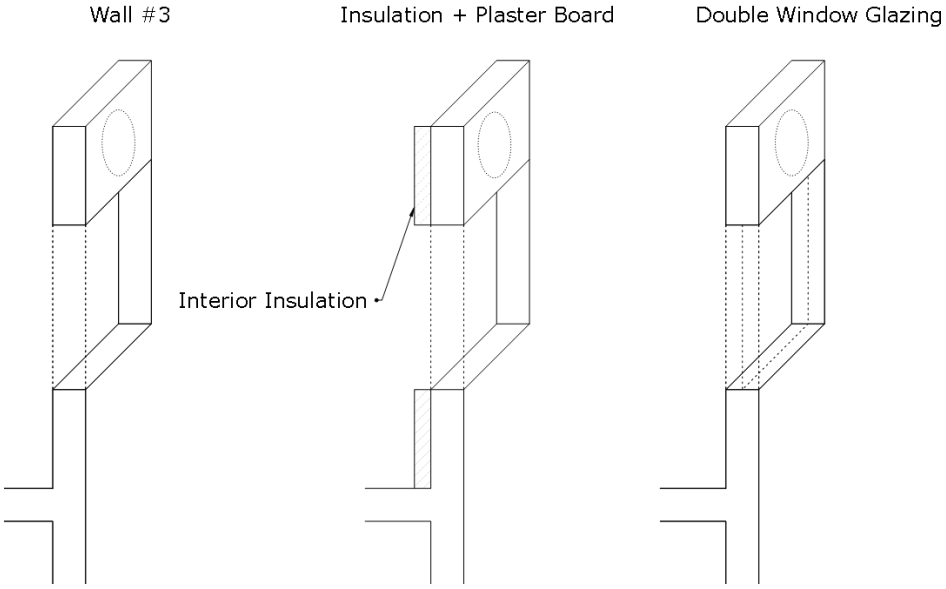

Figure 5 Bachoura Enhancement Scenarios

CHAPTER IV

GOVERNING EQUATIONS

A. Heat Transfer

The walls of a building are thermal interfaces that separate the indoor environment from the prevalent climate conditions of the outdoors. Heat enters and exists in the indoor space following the transient Fourier equation through the walls and the windows (Asan, 2006; Kaviany & Kanury, 2002). Three modes of heat transfer occur on the building wall. Initially, convection heat transfer occurs at both sides of the wall, as heat is transferred from the outside air to the wall and from the wall to the indoor space. In addition, radiation heat transfer is present on the outside surface of the wall due to its exposure to sunlight. Finally, all the heat received from the outdoor passes through the walls by thermal conduction. This thermodynamic phenomenon can be represented by the following system of equations:

$$k\frac{\partial^2 T}{\partial x^2} = \rho c_P \frac{\partial T}{\partial t} \; or \; \frac{\partial^2 T}{\partial x^2} = \frac{1}{\alpha}\frac{\partial T}{\partial t}$$

This equation is called the Fourier heat equation where k, ρ, c_p and $\alpha = \frac{k}{\rho c_p}$ are the conductivity, density, the specific heat, and the diffusivity of the material. The Fourier equation represents the transient heat transfer through the building material, while the convection and radiation modes of heat transfer is represented by the boundary conditions. By defining an x axis going from the inside to the outside of the wall, the following boundary conditions are formulated (Al-Sanea, 2000; Asan, 2006; Kaviany & Kanury, 2002):

$$k\left(\frac{\partial T}{\partial x}\right)_{x=0} = h_{\mathrm{i}}[T_{x=0}(t) - T_{\mathrm{i}}]$$

$$k\left(\frac{\partial T}{\partial x}\right)_{x=L} = h_o[T_o(t) - T_{x=L}(t)] + \lambda I_s + q_{r,o}$$

In these equations h_i, T_i and h_o, T_o are the surface heat transfer coefficient and the corresponding space temperature of the indoor and outdoor environments. λ is the solar absorptivity of the wall typically taken as 0.4 for light colored walls, I_s is the solar irradiance hitting the wall and $q_{r,o}$ is the radiation heat transfer between the wall and the sky given by the following equation:

$$q_{r,0} = \varepsilon\left(T_{sky}^4 - T_{x=L}^4\right)$$

Typically, the surface emissivity of the building materials ε is assumed to be 0.9 while T_{sky} is approximated as $T_{sky} = T_o - 12$ (Al-Sanea, 2000; Asan, 2006; Kaviany & Kanury, 2002).

Since this study aims to assess and improve the thermal comfort of existing buildings with unknown thermal properties of their materials, it may be useful to express the heat equation in a dimensionless form. In this analysis, the following parameters are defined: the dimensionless temperature θ, the dimensionless x coordinate ξ, and the dimensionless time coordinate τ. These parameters are defined as follows:

$$\theta = \frac{T}{T_r}, \xi = \frac{x}{L_r}, \tau = \frac{t}{t_r}$$

Where T_r, L_r, and t_r are chosen reference values for the temperature, length, and time, respectively. These values may seem arbitrary, however, the choice of the references values must lead to dimensionless parameters that range between zero and one (Kaviany & Kanury, 2002). The dimensionless heat equation is obtained by substituting these variables in the original equation:

$$\frac{\partial^2 \theta}{\partial \xi^2} = \frac{L_r^2}{\alpha t_r}\frac{\partial \theta}{\partial \tau}$$

The dimensionless form of the heat transfer equation highlights an important dimensionless group called the Fourier number Fo. First introduced by Jean Baptiste Joseph Fourier, this number represents the proportion of the heat conduction through the system compared to the energy stored within the system (Kaviany & Kanury, 2002).

$$\mathrm{Fo} = \frac{\alpha t_r}{L_r^2} = \frac{(k/L_r)}{\left(\rho c_p L_r / t_r\right)}$$

Knowing that the Nusselt number is $Nu = \frac{hL}{k_{air}}$, the boundary conditions in the new coordinate system are:

$$\left(\frac{\partial\theta}{\partial\xi}\right)_{\xi=0} = Nu_i[\theta_{\mathrm{x=0}}(t) - \theta_i(t)]$$

$$\left(\frac{\partial\theta}{\partial\xi}\right)_{\xi=1} = Nu_o[\theta_{\mathrm{o}}(t) - \theta_{x=L}(t)] + \frac{\lambda T_r}{k_{air}L_r} I_s$$

At ambient temperatures, the radiation heat flux can be neglected without compromising the accuracy of the models. While the solar irradiance heat flux is represented by the dimensionless expression $\frac{\lambda T_r}{k_{air}L_r} I_s$.

In a building with no air conditioning systems, free convection is present on both surfaces of the walls. Therefore, the Nusselt number can be directly correlated to the Rayleigh number which is given by(Kaviany & Kanury, 2002):

$$\mathrm{Ra} = \frac{l^2/\alpha}{\eta/\Delta\rho l g} = \frac{\Delta\rho l^3 g}{\eta\alpha} = \frac{\rho\beta\Delta T l^3 g}{\eta\alpha}$$

$$\bar{\mathrm{Nu}}_L = 0.68 + \frac{0.663\mathrm{Ra}_L^{1/4}}{[1 + (0.492/\mathrm{Pr})^{9/16}]^{4/9}} \quad \mathrm{Ra}_L \leq 10^8$$

Where:

- $Pr = \frac{c_p \mu}{k}$ is the Prandtl number.
- $\beta = -\frac{1}{\rho}\frac{\partial\rho}{\partial T}$.

- η is the kinematic viscosity.

Building Energy Simulations rely on a complex set of equations and elements that are not listed in this paper. However, the 1-D heat equation is enough to estimate the thermal properties of the building material (Al-Sanea, 2000; Asan, 2006; C1155 - 95 ASTM, 2013).

B. Bayesian Inferencing

Bayesian inferencing is the result of the conditional probability theory where it can evaluate the uncertainty of an unknown parameter M given an observation D. Bayes' rule relates the posterior conditional probability of the uncertain parameter $P(M|D)$ to the prior conditional probability of the same parameter $P(M)$ through the following formula (Yi et al., 2019):

$$P(M \mid D) \approx P(M)l(D \mid M)$$

Where:

- M is the uncertain parameter.
- D is the observed data.
- $P(M \mid D)$ is the posterior probability distribution.
- $P(M)$ is the prior probability distribution.
- $l(D \mid M)$ is the likelihood of having the set of data D given the parameter M.

In this analysis, the choice of the prior distribution greatly affects the inferencing algorithm. The choice of such distribution is entirely left to the researcher and may vary from one researcher to the other based on their personal experience. Yi et al., (2019) distinguish between two types of prior probability distributions which are the informative prior and the uninformative prior. The informative prior, say a Gaussian distribution, has the probability of predicting the output value of the model. On the

other hand, the uninformative distribution, say a uniform distribution, does not predict such output as it applies an equal weighting to all its parameters.

The likelihood $l(D|M)$ is a function of the observed data corresponding to each parameter. This factor does not depend on the choice made by the researcher as it has a corresponding formula for the chosen probability distribution. If the data follows a Gaussian distribution, the likelihood is given by:

$$D = f(M) + \mathrm{e}$$
$$l(D|M) \propto \exp\left\{-\frac{1}{2}(D - f(M))^T C^{-1}(D - f(M))\right\}$$

Where:

- $f(M)$ is the simulation model output.
- e is the error present in the model.
- C is the covariance matrix of the model.

Usually, in Bayesian statistical analysis, this inferencing algorithm is used along with the Markov Chain Monte Carlo method (MCMC) to probabilistically determine the model inputs. On this basis thousands of samples are drawn from the chosen probability distribution and based on the calculated likelihood a sample is either accepted or rejected, constructing a Markov chain (Chong et al., 2015; Yi et al., 2019).

C. Thermal Comfort Estimation

As discussed previously, thermal comfort calculations differ depending on the type of ventilation in the occupied space. In mechanically ventilated spaces, thermal comfort is based on the PMV model where the emphasis is on the indoor temperature and the heat transfer between the person and the surrounding. However, this model fails in naturally ventilated spaces. ASHRAE addresses these flaws by introducing adaptive thermal comfort in the standard ASHRAE-55 (Turner et al., 2010). The adaptive

ASHRAE-55 model is one of the many thermal comfort models available in the OpenStudio application. Therefore, it was selected as the basis of thermal comfort calculations in the four studied spaces This model states that, in naturally ventilated spaces, the occupant's sensation of comfort is a function of the outdoor temperature, clothing insulation, window operation schedule, activity schedule, metabolic rate, airspeed, and humidity.

1. Model parameters

ASHRAE-55 defines a naturally ventilated building as the space where the indoor thermal conditions are regulated by the occupants through the operation of the windows. The following are the main parameters included in the model calculation.

a. Clothing insulation (I_{cl}):

Defined as the thermal resistance to the sensible heat transfer provided by the clothing worn by the occupants. It is usually expressed in clothing units (clo). The clo value includes the parts of the body not covered in any cloth such as the head or hands.

b. Mean Radiant Temperature (T_r):

Refers to the uniform surface temperature of an imaginary black box enclosure where the radiant heat transferred by the occupants is the same as the one in the non-uniform space.

c. Prevailing Mean Outdoor Air Temperature ($\overline{t_{pma(out)}}$)

A main input of the adaptive ASHRAE-55 thermal comfort model, this temperature is based on the average daily outdoor temperature over a certain period.

d. Operative Temperature(t_o):

Refers to the uniform surface temperature of an imaginary black box enclosure where the radiative and convective heat that is transferred by the occupants is the same as the one in the non-uniform space.

2. Thermal Comfort Calculation

a. Clothing Insulation:

In a naturally conditioned space, clothing is the main way by which the occupants react to the changes in the outdoor conditions. Usually, clothing insulation is given a value of 0.5 for the summer conditions and a value of 1 for the winter conditions. For near sedentary activities clothing insulation values affect the operative indoor temperature by a factor of $6℃/clo$:

$$t_{o,adaptive} = t_o \pm I_{clo} \times 6℃/clo$$

b. Mean Radiant Temperature:

This temperature is derived from the temperature of the surfaces surrounding a person and the angle factor between the person and those surfaces:

$$\bar{T}_{\mathrm{r}}^4 = T_1^4 F_{p\to 1} + T_2^4 F_{p\to 2} + \cdots + T_i^4 F_{p\to i} + \cdots + T_N^4 F_{p\to N}$$

The angle factor is a function of the surface geometry: height a, width b, and the distance c between the person and the said surface:

$$F_{p-i} = F_{\max}\left[1 - \mathrm{e}^{-(a/c)/\tau}\right]\left[1 - \mathrm{e}^{-(b/c)/\gamma}\right]$$

Where:

$$\tau = A + B(a/c)$$

$$\gamma = C + D(b/c) + E(a/c)$$

The variables F_{max}, A, B, C, D, and E are a function of the occupants' activity such as the person being seated or standing. This model can be simplified if there is a small difference between the surface temperatures of the enclosure.

$$\bar{T}_{\mathrm{r}} = T_1 F_{p\to 1} + T_2 F_{p\to 2} + \cdots + T_i F_{p\to i} + \cdots + T_N F_{p\to N}$$

c. Operative Temperature:

It is calculated as the weighted average of the indoor air temperature and the mean radiant temperatures. These values are weighted by the heat transfer coefficient and the linearized radiant heat transfer coefficient for the occupants. ASHRAE-55 deems it acceptable to approximate the operative temperature as follows:

$$t_o = (t_a + t_r)/2$$

Where:

- $t_o =$ operative temperature,
- $t_a =$ air temperature, and
- $t_r =$ mean radiant temperature.

d. Acceptable Temperature Limit:

The acceptable range of operative temperatures is defined by the following equations and reflected in Figure 5.

$$\text{Upper 80\% acceptability limit } (^\circ\mathrm{C}) = 0.31\overline{t_{pma(out)}} + 21.3$$

$$\text{Lower 80\% acceptability limit } (^\circ\mathrm{C}) = 0.31\overline{t_{pma(out)}} + 14.3$$

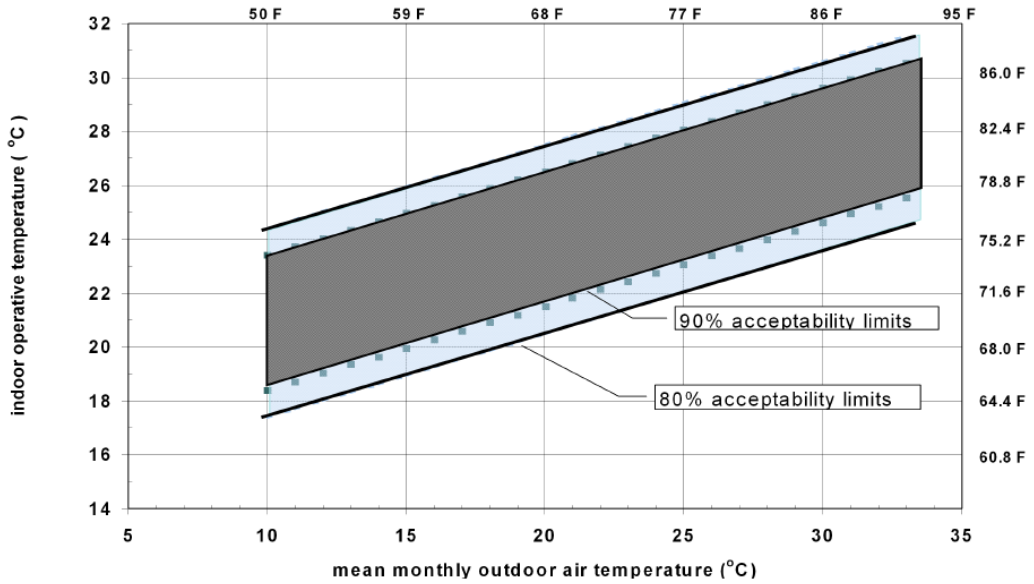

Figure 6 Acceptable Operating Temperatures

e. Time not Comfortable under ASHRAE-55:

It is the sum of all the operational hours where the operative temperature falls outside the 80% acceptability limit. This value is used to quantify the thermal discomfort felt by the occupants during the typical methodological year (TMY).

CHAPTER V

RESULTS AND DISCUSSION

A. Thermal Behavior

The thermal behavior of the wall is first assessed using the time lag and decrement factors. The unsteady state conditions of the measured data are reflected in the irregularities in the values. A comparison between the raw data and the output of the FFT analysis is made in the following figures:

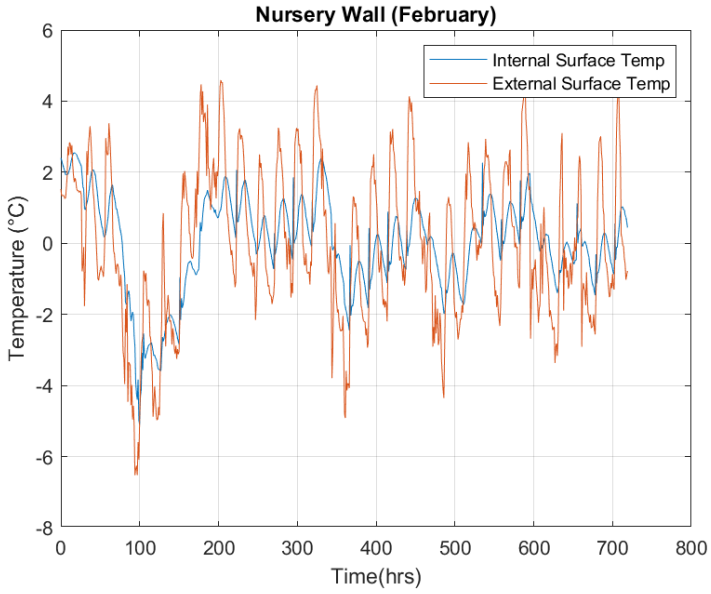

Figure 7 Temperature Variation of the Nursery Wall for the Month of February

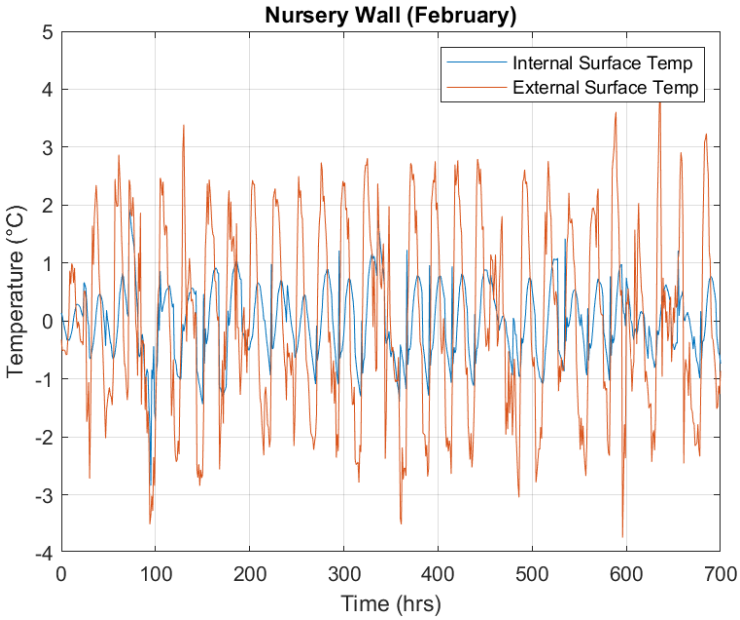

Figure 8 Temperature of the Nursery Wall for the Month of February after Subtracting the Average Daily Temperature

The unsteady state nature of the measurements is apparent in Fig 6. A sharp decline in the temperature curve represents the building's response to sudden cold shifts in the weather. Moreover, the data in Fig 6 have a noticeable baseline shift which affects the calculation process. The transformed data in Fig 7 is aligned with the x-axis which provides a consistent basis for the calculation of the thermal time lag. The decrement factor is unaffected by this transformation. For the Nursery wall, the average thermal time lag increases when the outdoor conditions are comfortable. While the decrement factor is the highest in the coldest climate. These values along with the variations in the temperature values throughout the years indicate that the thermal comfort in the class is achieved when the outdoor temperatures are in the comfort range mostly in the early fall and spring seasons. This building struggles to maintain the indoor temperatures at a comfortable range when the outdoor is too hot or too cold.

For the Bachoura wall, that is facing a tree, the fluctuation of the inside and outside surface temperatures is minimal. While the inside surface temperature and the outside surface temperatures are nearly equal, the heat flux is the lowest compared to the other walls. The average thermal time lag is the highest among the studied walls. It has a consistent behavior during the hot and the cold climates. For the Bachoura wall, which is not facing a tree, the variance in its temperature and heat flux values is the highest. Concerning the thermal time lag and decrement factor, they follow a similar trend as one of the Nursery walls. Thermal comfort is achieved in an adequate climate while the spaces become uncomfortable in extreme conditions.

Table 4 Thermal time lag and decrement factor

Studied Wall	Month	Thermal Time Lag (hrs.)	Decrement Factor
Nursery	February	3.66	0.39
	April	5.09	0.29
	July	4.33	0.29
Khaled	February	2.8	0.49
	April	5.2	0.44
	August	3.6	0.5
Bachoura (Tree)	November	6.11	0.46
	October	4.21	0.423
	August	6.4	0.40

B. Building Energy Modeling and Bayesian Inferencing

The building energy models for the four spaces were made using the OpenStudio application and the known construction properties of the sandstone and concrete walls and the geometry of the corresponding spaces. Figures 9,10 and 11 represent the model geometry that corresponds to each space.

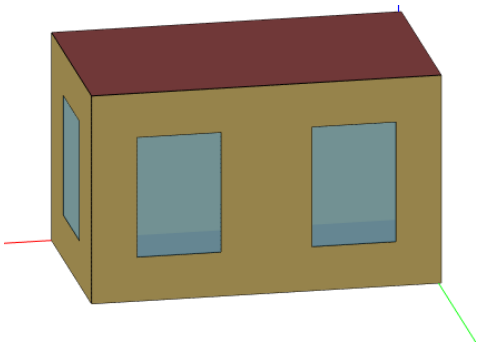

Figure 9 Geometry of the Nursery Space

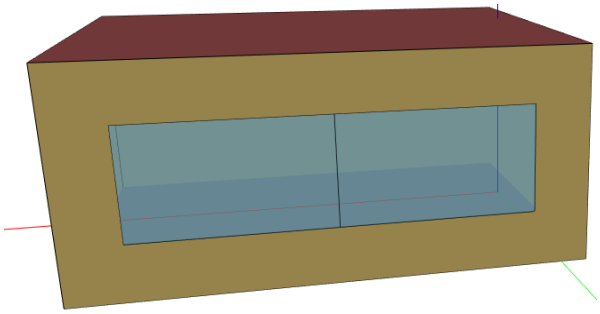

Figure 10 Geometry of the Khaled Space

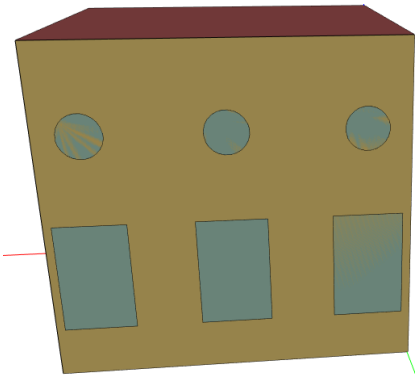

Figure 11 Geometry of the Bachoura Space (No Tree)

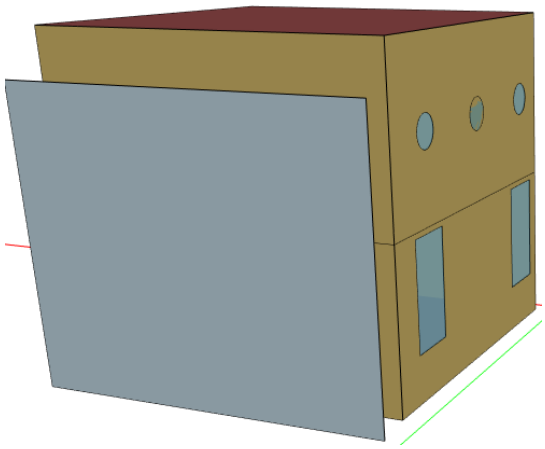

Figure 12 Geometry of the Bachoura Space (Tree)

The EnergyPlus base file was introduced in the MCMC algorithm to get a posterior distribution of the $\rho_1 c_1$ product for the concrete. The density heat product for the sandstone walls was designated by $\rho_2 c_2$. The density and the specific heat of the concrete cannot be calculated separately as the model outputs the same temperatures for the same ρc product. For the Nursey wall, the results of the Bayesian inferencing algorithm are shown in Figure 13.

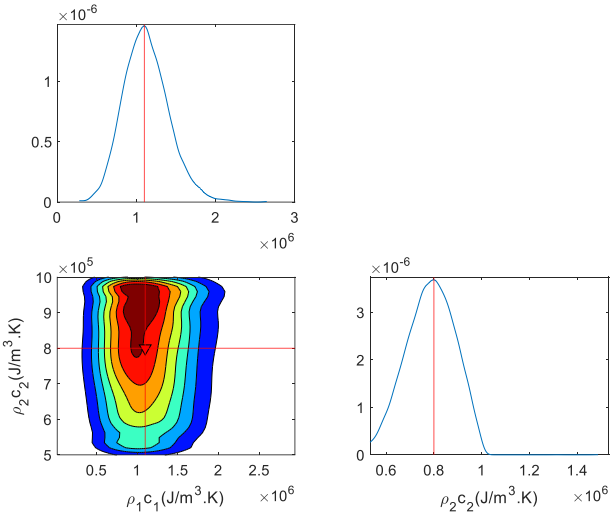

Figure 13 Corner plot for Concrete (1) and Sandstone (2)

The output of the algorithm was validated against the real value of $\rho_2 c_2$ which is $0.85 \times 10^6\ J/m^3K$. The concrete was found to have a density heat product $\rho_1 c_1 = 1.1 \times 10^6\ J/m^3K$. The resulting model has an error $CVRMSE = 4\%$ and $NMBE = 3\%$ which are within the calibration limits set by ASHRAE. The procedure was repeated for the remaining spaces and its results are summarized in Table 5.

Table 5 Error Percentage for the Calibrated Models

Space Studied	CVRMSE (%)	NMBE (%)
Space 1	3.1	4.3
Space 2	5.4	7.5
Space 3a	6.3	5.5
Space 3b	7.2	6.5

C. Thermal Comfort Assessment and Enhancement

Since the spaces were naturally conditioned, thermal comfort was assessed based on the adaptive AHRAE-55 model. In the simulation report, the OpenStudio application groups the simulated temperature in specific intervals representing the hot, neutral, and cold climate conditions respectively as shown in the Appendix. A general conclusion from this classification is that these spaces perform poorly under high heat and thermal stress. Furthermore, the effect of the shading provided by the tree in front of Wall 3a is apparent by comparing those results. Compared to the non-shaded Bachoura space, the shaded one has the highest heat resistance and performs the best under thermal stress. It also performs better under cold conditions, which is consistent with the results reported by Haggag et al., (2017). Trees can shield the wall from solar radiation and also provide a shield from the cold winter wind. It is also apparent that the Khaled space has the worst response to the summer heat, as it spends more than 2000 hours in temperatures

greater than 30℃. These results are to be expected as hollow concrete blocks have low thermal resistance and are designed to be cheap and practical rather than to account for thermal comfort (Hema et al., 2020; Sassine et al., 2020; Uriarte-Flores et al., 2019).

1. Thermal comfort Assessment

The results of the adaptive thermal comfort assessment of the four spaces are as follows:

- The Nursery space had $3588\ hrs$ of uncomfortable thermal conditions.
- The Khaled space had $4065 hrs$ of uncomfortable thermal conditions, notably the highest among the studied spaces.
- The Bachoura space, not shielded by a tree, had $3420\ hrs$ of uncomfortable thermal conditions.
- The Bachoura space, shielded by a tree, had $3300\ hrs$ of uncomfortable thermal conditions, notably the least among all the studied spaces.

The U-value of the studied walls are summarized in Table 6:

Table 6 U-value of the Studied Spaces

	Wall #1	**Wall #2**	**Wall #3**
U-Value $(\boldsymbol{W/m^2K})$	1.32	1.49	0.96

The spaces with the sandstone construction have a better record of thermal comfort under the Adaptive ASHRAE-55 than the one with concrete construction. These results are backed by both experimental data and the literature. Wall #2 has the highest U-value among the four walls. Furthermore, when comparing the performance of hollow concrete blocks with stone, bricks, and similar constructions with high thermal mass,

these materials provide better thermal comfort in both hot and cold climates (Homod et al., 2021; Hema et al., 2020).

2. Thermal Comfort Enhancement

The enhancement scenarios were run in the OpenStudio application and the results of the comparison of the different insulation materials are shown in Tables 7 and 8, while the comparison between the best options from each category is shown in Table 9. The studied spaces can be classified based on the thermal mass of the opaque envelope. The simulation results show that:

- The Nursery space benefits the most from an external XPS insulation as it reduces the uncomfortable hours from 3588 to 2600, and the double window glazing had a small but noticeable impact on the indoor thermal comfort. This space has a volume of $101.35\ m^3$, outdoor wall area of $25.22\ m^2$ and window to wall ratio of 27.75% in the North direction, 23.6% in the East direction and 13.11% in total.
- The Khaled space benefits the most from an external XPS insulation as it reduces the uncomfortable hours from 4065 to 2500, and the double window glazing is essential in reducing the uncomfortable hours from 2500 to 1950. This space has a volume of 146.52 m^3 and outdoor wall area of $11.1m^2$ and window to wall ratio of 38.28% in the north direction and 10.57%.
- The Bachoura spaces have the restriction that outdoor insulation cannot be placed to preserve the outdoor architecture of the building. This space benefits the most from either stone wool insulation or XPS which reduces the uncomfortable hours from 3420 to 2350. The shading provided by the tree and the low window to wall ratio resulted in the negligible effect of the double

window glazing on indoor thermal comfort. These spaces have a similar geometry with a window to wall ratio of 10.3% on the north wall, 10.68% on the west wall, and a 5.17% in total.

Table 7 Uncomfortable Hours for Different Internal Insulations For One Year

Space	Base Model	Total Hours	Cork	EP	XPS	Stone Wool	Best Choice
Nursery	3588	8000	2890	2850	2800	2650	XPS
Khaled	4065	8000	3700	3100	3000	3850	EP/XPS
Bachoura (Tree)	3420	8000	2812	2800	2200	2400	Stone Wool/XPS
Bachoura (No Tree)	3300	8000	2721	2615	2250	2312	Stone Wool/XPS

Table 8 Uncomfortable Hours for Different External Insulations for One Year

Space	Base Model	Total Hours	Cork	EP	XPS	Stone Wool	Best Choice
Nursery	3588	8000	3120	2900	2700	3010	XPS
Khaled	4065	8000	3513	2700	2500	2850	XPS

Table 9 Uncomfortable Hours Comparison Between all Scenarios for One Year

Space	Base Model	Total Hours	Indoor Insulation	Outdoor insulation	Best Choice +Double Window Glazing	Final Choice
Nursery	3588	8000	2850	2600	2420	Outdoor XPS
Khaled	4065	8000	3000	2500	1950	Outdoor XPS+ Double Window glazing
Bachoura (No Tree)	3420	8000	2500	NA	2390	Stone Wool
Bachoura (Tree)	3300	8000	2412	NA	2310	Stone Wool

The spaces of the Nursery and Bachoura have an envelope made from high thermal mass sandstone. While the Khaled space is made from low thermal mass hollow concrete blocks. This distinction is important in studying the effect of adding insulations on the thermal comfort of the buildings. For naturally ventilated buildings, internal insulation may worsen the indoor conditions in high thermal mass spaces such as brick or stone walls while the spaces with low thermal mass respond better to this type of insulation (Hashemi, 2017). This observation explains why the Nursery and Bachoura spaces limited benefits from the addition of internal insulation. External insulation has proven to be consistently better than indoor ones as backed by the simulation results and Hashemi (2017). For the Khaled space, two main factors controlled the thermal comfort indoors: the window to wall ratio and the low thermal mass of concrete. The Khaled space has the highest window to wall ratio on the outdoor wall, therefore the U- value of the windows has a great effect on the thermal comfort in the classroom. This is further supported by the literature as in walls with a high window to wall ratio, the U-value of the windows dictates the heat transfer between the façade and the outdoors (Alwetaishi, 2019; Potrč Obrecht et al., 2019). For the Bachoura spaces, the effect of the shading provided by the tree makes any modification of the current windows setup pointless. Furthermore, these spaces benefitted the most from a stone wall insulation as it has the best combination between thermal mass and thermal resistance.

CHAPTER VI

CONCLUSION

In this study, retrofit strategies were proposed to enhance the thermal comfort of four different spaces in the Makassed schools. Energy models for these spaces were made using the OpenStudio application and calibrated using the Markov Chain Monte Carlo Method. The results of the calibration proved the capability of the MCMC algorithm to predict the uncertain variables in the existing buildings. The resulting models all complied with the ASHRAE standard as the error coefficients ranged from 3 to 7%. In summary, the following modification was proposed for the studied spaces:

- For the Nursery space, an external XPS insulation coupled with a double window glazing as it reduced the uncomfortable hours by 33%.
- For the Khaled space, an external XPS insulation coupled with a double window glazing as it reduced the uncomfortable hours by 52%.
- For the Bachoura space, internal stone-wool insulation as it reduced the uncomfortable hours by 30%.

A notable limitation of this study is that the four spaces were studied as separate units, approximating the interaction between each classroom and the building using the boundary conditions. Future studies need to address the effect of studying the thermal behavior of the space in context to its surroundings. For instance, in large cities, the urban island heat effect may alter the thermal behavior of the walls in a way that can not be replicated in simple energy modeling.

APPENDIX

Operational Temperature Classification

1. Nursery

Temperature (Table values represent hours spent in each temperature range)

Zone	Unmet Htg (hr)	Unmet Htg - Occ (hr)	< 13 (C)	13-16 (C)	16-18 (C)	18-20 (C)	20-21 (C)	21-22 (C)	22-23 (C)	23-24 (C)	24-26 (C)	26-28 (C)	28-30 (C)	>= 30 (C)	Unmet Clg (hr)	Unmet Clg - Occ (hr)	Mean Temp (C)
THERMAL ZONE 1	0	0	15	215	623	676	400	457	456	377	871	1075	1309	1206	0	0	24.8 (C)

Figure 14 Temperature Classification for the Nursery Space

2. Khaled

Temperature (Table values represent hours spent in each temperature range)

Zone	Unmet Htg (hr)	Unmet Htg - Occ (hr)	< 13 (C)	13-16 (C)	16-18 (C)	18-20 (C)	20-21 (C)	21-22 (C)	22-23 (C)	23-24 (C)	24-26 (C)	26-28 (C)	28-30 (C)	>= 30 (C)	Unmet Clg (hr)	Unmet Clg - Occ (hr)	Mean Temp (C)
THERMAL ZONE 1	0	0	0	59	505	710	387	411	468	592	1161	1096	1050	2321	0	0	26.3 (C)

Figure 15 Temperature Classification for the Khaled Space

3. Bachoura (Tree)

Temperature (Table values represent hours spent in each temperature range)

Zone	Unmet Htg (hr)	Unmet Htg - Occ (hr)	< 13 (C)	13-16 (C)	16-18 (C)	18-20 (C)	20-21 (C)	21-22 (C)	22-23 (C)	23-24 (C)	24-26 (C)	26-28 (C)	28-30 (C)	>= 30 (C)	Unmet Clg (hr)	Unmet Clg - Occ (hr)	Mean Temp (C)
THERMAL ZONE 1	0	0	0	54	2253	1656	550	760	637	732	2042	76	0	0	0	0	20.9 (C)
THERMAL ZONE 1 PLENUM	0	0	15	2452	1406	989	660	406	691	1022	1119	0	0	0	0	0	19.3 (C)

Figure 16 Temperature Classification for the Bachoura Space

4. Bachoura (No tree)

Temperature (Table values represent hours spent in each temperature range)

Zone	Unmet Htg (hr)	Unmet Htg - Occ (hr)	< 13 (C)	13-16 (C)	16-18 (C)	18-20 (C)	20-21 (C)	21-22 (C)	22-23 (C)	23-24 (C)	24-26 (C)	26-28 (C)	28-30 (C)	>= 30 (C)	Unmet Clg (hr)	Unmet Clg - Occ (hr)	Mean Temp (C)
THERMAL ZONE 1	0	0	753	1851	1096	794	355	439	503	763	1310	828	63	5	0	0	19.7 (C)

Figure 17 Temperature Classification for the Bachoura Space (No Tree)

REFERENCES

Al-Sanea, S. A. (2000). Evaluation of Heat Transfer Characteristics of Building Wall Elements. *Journal of King Saud University - Engineering Sciences*, *12*(2), 285–312. https://doi.org/10.1016/S1018-3639(18)30720-7

Albatayneh, A., Alterman, D., Page, A., & Moghtaderi, B. (2018). The impact of the thermal comfort models on the prediction of building energy consumption. *Sustainability (Switzerland)*, *10*(10). https://doi.org/10.3390/su10103609

Alwetaishi, M. (2019). Impact of glazing to wall ratio in various climatic regions: A case study. *Journal of King Saud University - Engineering Sciences*, *31*(1), 6–18. https://doi.org/10.1016/j.jksues.2017.03.001

Asan, H. (2006). Numerical computation of time lags and decrement factors for different building materials. *Building and Environment*, *41*(5), 615–620. https://doi.org/10.1016/j.buildenv.2005.02.020

Babu, A., Puttaranga, T., & Shaik, S. (2014). *Study of Unsteady State Thermal Characteristics of Homogeneous and Composite Walls of Building and Insulating Materials for Passive Cooling*. 1–10.

Bagnasco, A., Massucco, S., Saviozzi, M., Silvestro, F., & Vinci, A. (2018). Design and Validation of a Detailed Building Thermal Model Considering Occupancy and Temperature Sensors. *IEEE 4th International Forum on Research and Technologies for Society and Industry, RTSI 2018 - Proceedings*, 1–6. https://doi.org/10.1109/RTSI.2018.8548424

Bevilacqua, P., Mazzeo, D., & Arcuri, N. (2018). Thermal inertia assessment of an experimental extensive green roof in summer conditions. *Building and Environment*, *131*(November 2017), 264–276. https://doi.org/10.1016/j.buildenv.2017.11.033

Brackney, L., Parker, A., Macumber, D., & Benne, K. (2018). Building Energy Modeling with OpenStudio. In *Building Energy Modeling with OpenStudio*. https://doi.org/10.1007/978-3-319-77809-9

C1155 - 95 ASTM. (2013). Standard Practice for Determining Thermal Resistance of Building Envelope Components from the In-Situ Data. *Astm*, *i*(Reapproved 2007), 1–8. https://doi.org/10.1520/C1155-95R13.2

Cherier, M. K., Benouaz, T., Bekkouche, S. M. A., Hamdani, M., & Djeffal, R. (2019). Improvement temperatures of a studio apartment through judicious choice of materials and eco building materials under an arid climate - Case study Ghardaïa. *IOP Conference Series: Earth and Environmental Science*, *214*(1). https://doi.org/10.1088/1755-1315/214/1/012118

Chong, A., Xu, W., & Lam, K. P. (2015). UNCERTAINTY ANALYSIS IN BUILDING ENERGY SIMULATION : A PRACTICAL APPROACH Center for Building Performance and Diagnostics , Carnegie Mellon University , Pittsburgh , USA. *Building Simulation Conference*, 2796–2803.

Corrado, V., & Mechri, H. E. (2009). Uncertainty and sensitivity analysis for building energy rating. *Journal of Building Physics*, *33*(2), 125–156. https://doi.org/10.1177/1744259109104884

Gasparella, A., Pernigotto, G., Baratieri, M., & Baggio, P. (2011). Thermal dynamic transfer properties of the opaque envelope : Analytical and numerical tools for the assessment of the response to summer outdoor conditions. *Energy & Buildings*,

43(9), 2509–2517. https://doi.org/10.1016/j.enbuild.2011.06.004
Haggag, M., Hassan, A., & Qadir, G. (2017). Energy and economic performance of plant-shaded building Façade in hot arid climate. *Sustainability (Switzerland)*, *9*(11). https://doi.org/10.3390/su9112026
Hashemi, A. (2017). Effects of thermal insulation on thermal comfort in low-income tropical housing. *Energy Procedia*, *134*, 815–824. https://doi.org/10.1016/j.egypro.2017.09.535
Hema, C., Messan, A., Lawane, A., & Van Moeseke, G. (2020). Impact of the Design of Walls Made of Compressed Earth Blocks on the Thermal Comfort of Housing in Hot Climate. *Buildings*, *10*(9), 157. https://doi.org/10.3390/buildings10090157
Homod, R. Z., Almusaed, A., Almssad, A., Jaafar, M. K., Goodarzi, M., & Sahari, K. S. M. (2021). Effect of different building envelope materials on thermal comfort and air-conditioning energy savings: A case study in Basra city, Iraq. *Journal of Energy Storage*, *34*(October), 101975. https://doi.org/10.1016/j.est.2020.101975
Jannat, N., Hussien, A., Abdullah, B., & Cotgrave, A. (2020). A comparative simulation study of the thermal performances of the building envelope wall materials in the tropics. *Sustainability (Switzerland)*, *12*(12). https://doi.org/10.3390/SU12124892
Jradi, M., Veje, C., & Jørgensen, B. N. (2017). Deep energy renovation of the Mærsk office building in Denmark using a holistic design approach. *Energy and Buildings*, *151*(2017), 306–319. https://doi.org/10.1016/j.enbuild.2017.06.047
Kaviany, M., & Kanury, A. (2002). Principles of Heat Transfer. In *Applied Mechanics Reviews* (Vol. 55, Issue 5). https://doi.org/10.1115/1.1497490
Kumar, G. K., Saboor, S., & Babu, T. P. A. (2017). Study of Various Glass Window and Building Wall Materials in Different Climatic Zones of India for Energy Efficient Building Construction. *Energy Procedia*, *138*, 580–585. https://doi.org/10.1016/j.egypro.2017.10.163
Latha, P. K., Darshana, Y., & Venugopal, V. (2015). Role of building material in thermal comfort in tropical climates - A review. *Journal of Building Engineering*, *3*, 104–113. https://doi.org/10.1016/j.jobe.2015.06.003
Nicol, J. F., & Humphreys, M. A. (2002). Adaptive thermal comfort and sustainable thermal standards for buildings. *Energy and Buildings*, *34*(6), 563–572. https://doi.org/10.1016/S0378-7788(02)00006-3
Potrč Obrecht, T., Premrov, M., & Žegarac Leskovar, V. (2019). Influence of the orientation on the optimal glazing size for passive houses in different European climates (for non-cardinal directions). *Solar Energy*, *189*(June), 15–25. https://doi.org/10.1016/j.solener.2019.07.037
Prada, A., Pernigotto, G., Baggio, P., & Gasparella, A. (2018). Uncertainty propagation of material properties in energy simulation of existing residential buildings: The role of buildings features. *Building Simulation*, *11*(3), 449–464. https://doi.org/10.1007/s12273-017-0418-4
Sassine, E., Cherif, Y., Dgheim, J., & Antczak, E. (2020). Experimental and Numerical Thermal Assessment of Lebanese Traditional Hollow Blocks. *International Journal of Thermophysics*, *41*(4). https://doi.org/10.1007/s10765-020-02626-7
Toure, P. M., Dieye, Y., Gueye, P. M., Sambou, V., Bodian, S., & Tiguampo, S. (2019). Experimental determination of time lag and decrement factor. *Case Studies in Construction Materials*, *11*, e00298. https://doi.org/10.1016/j.cscm.2019.e00298
Turner, S. C., Paliaga, G., Lynch, B. M., Arens, E. A., Aynsley, R. M., Brager, G. S., Deringer, J. J., Ferguson, J. M., Filler, J. M., Hogeling, J. J., Int-hout, D., Kwok, A.

G., Levy, H. F., Sterling, E. M., Stoops, J. L., Taylor, S. T., Tinsley, R. W., Cooper, K. W., Dean, K. W., … Peterson, J. C. (2010). American society of heating, refrigerating and air-conditioning engineers. *International Journal of Refrigeration*, *2*(1), 56–57. https://doi.org/10.1016/0140-7007(79)90114-2

Uriarte-Flores, J., Xamán, J., Chávez, Y., Hernández-López, I., Moraga, N. O., & Aguilar, J. O. (2019). Thermal performance of walls with passive cooling techniques using traditional materials available in the Mexican market. *Applied Thermal Engineering*, *149*(December 2018), 1154–1169. https://doi.org/10.1016/j.applthermaleng.2018.12.045

Yi, D. H., Kim, D. W., & Park, C. S. (2019). Parameter identifiability in Bayesian inference for building energy models. *Energy and Buildings*, *198*, 318–328. https://doi.org/10.1016/j.enbuild.2019.06.012